Glycobiology vol. 21 no. 5 pp. 634–643, 2010
doi:10.1093/glycob/cwq211
Advance Access publication on December 24, 2010

N-Glycans mutations rule oligomeric assembly and functional expression of $P2X_3$ receptor for extracellular ATP

Fabrizio Vacca[2,3,1], Nadia D'Ambrosi[2,4], Valeria Nestola[2], Susanna Amadio[2], Michela Giustizieri[5], Maria Letizia Cucchiaroni[5], Alessandro Tozzi[5], Marie Claire Velluz[3], Nicola Biagio Mercuri[5,6], and Cinzia Volonté[2,4]

[2]Laboratory Cellular Neurobiology, Santa Lucia Foundation, Via del Fosso di Fiorano 65, 00143 Rome, Italy; [3]Department of Biochemistry, University of Geneva, Genève 1211, Switzerland; [4]CNR Institute of Neurobiology and Molecular Medicine, and [5]Laboratory Experimental Neurology, Santa Lucia Foundation, Rome 00143, Italy; and [6]Department of Neuroscience, University of Rome "Tor Vergata", Rome 00143, Italy

Received on March 15, 2010; revised on December 13, 2010; accepted on December 14, 2010

N-Glycosylation affects the function of ion channels at the level of multisubunit assembly, protein trafficking, ligand binding and channel opening. Like the majority of membrane proteins, ionotropic P2X receptors for extracellular ATP are glycosylated in their extracellular moiety. Here, we used site-directed mutagenesis to the four predicted N-glycosylation sites of $P2X_3$ receptor (Asn^{139}, Asn^{170}, Asn^{194} and Asn^{290}) and performed comparative analysis of the role of *N*-glycans on protein stability, plasma membrane delivery, trimer formation and inward currents. We have found that in transiently transfected HEK293 cells, Asn^{170} is apparently the most important site for receptor stability, since its mutation causes a primary loss in protein content and indirect failure in membrane expression, oligomeric association and inward current responses. Even stronger effects are obtained when mutating Thr^{172} in the same glycosylation consensus. Asn^{194} and Asn^{290} are the most dispensable, since even their simultaneous mutation does not affect any tested receptor feature. All double mutants containing Asn^{170} mutation or the Asn^{139}/Asn^{290} double mutant are instead almost unable to assemble into a functional trimeric structure. The main emerging finding is that the inability to assemble into trimers might account for the impaired function in $P2X_3$ mutants where residue Asn^{170} is replaced. These results improve our knowledge about the role of N-glycosylation in proper folding and oligomeric association of $P2X_3$ receptor.

Keywords: αβmeATP / inward currents / oligomerization / proteasome inhibition / trafficking

Introduction

It is well known that N-glycosylation often affects the function of ion channels at the level of multisubunit assembly, protein trafficking, ligand binding and channel opening (Gehle et al. 1997; Standley and Baudry 2000; de Souza and Simon 2002; Gong et al. 2002; Watanabe et al. 2003). *N*-Linked glycans also exert a well-recognized role as maturation and quality-control tags in the early secretory pathway (Hebert et al. 2005). They are added co-translationally during the translocation in the lumen of the endoplasmic reticulum (ER; Kowarik et al. 2002) and mediate the recognition by the lectin chaperones, calnexin and calreticulin, which assist proper protein folding (Molinari and Helenius 2000; Daniels et al. 2003). The overall importance of glycosylation in membrane and secretory proteins has been further revealed by congenital disorders of glycosylation, which are multisystem syndromes causing various degrees of mental and psychomotor retardation and severely affecting humans (Freeze 2001; Jaeken and Carchon 2004).

P2X receptors constitute a family of seven ($P2X_{1–7}$) cation channels gated by extracellular ATP. They are expressed in many excitable and not excitable cells to mediate a variety of physiological actions, including smooth muscle contraction, neuroendocrine secretion and synaptic transmission (Khakh and North 2006). They have a membrane topology with two transmembrane domains and form functional homo- or heterotrimeric channels on the plasma membrane (PM; Nicke et al. 1998; Barrera et al. 2005). Among them, the $P2X_3$ subtype that we demonstrated to be enriched in specialized submembrane compartments such as lipid rafts (Vacca et al. 2004) is present in cell bodies as well as in peripheral and central terminals of sensory neurons of dorsal root ganglia (Vulchanova et al. 1997), where it performs a well-defined role in sensory and pain transmission (Cockayne et al. 2000; Souslova et al. 2000; North 2004). Like the majority of membrane proteins, all P2X receptors are glycosylated in their extracellular moiety. N-Glycosylation has been studied in several members of the P2X family: Asn-linked glycans in $P2X_1$ (Rettinger et al. 2000; Roberts and Evans 2006), $P2X_2$ (Torres et al. 1998), $P2X_4$ (Hu et al. 2002) and $P2X_6$ (Jones et al. 2004) receptor subtypes have been shown to affect several aspects of receptor function, including oligomerization, surface expression and

[1]To whom correspondence should be addressed: Tel: +39-06-501703084; Fax: +39-06-501703321; e-mail: fabrizio.vacca@unige.ch

channel function. Whereas the four consensus sequences (N-X-S/T) for N-linked glycosylation in the extracellular domain of $P2X_3$ receptor (Asn^{139}, Asn^{170}, Asn^{194} and Asn^{290}) are homologous to the four recognized N-glycosylation sites of $P2X_1$ receptor (Rettinger et al. 2000), there is only a partial homology with the number and position of *N*-glycans in all other P2X isoforms.

In a previous study, we demonstrated that $P2X_3$ receptor undergoes rapid constitutive endocytosis accompanied by preferential targeting to late endosomes/lysosomes with subsequent degradation (Vacca et al. 2009). In the present work, we used site-directed mutagenesis to investigate the role of *N*-glycans in $P2X_3$ receptor function. By means of transiently transfected HEK293 cells, we demonstrated an essential but heterogeneous role of *N*-glycan residues in overall protein expression, PM delivery, oligomerization and inward current response.

Results

Effect of single N-glycosylation site mutation on functional expression of P2X₃ receptor

In order to evaluate how the removal of individual *N*-glycans affects the functional expression of $P2X_3$ receptor, we produced N-glycosylation defective mutants by substituting Asn with Gln through site-directed mutagenesis in the four predicted N-glycosylation sites of the receptor (Asn^{139}, Asn^{170}, Asn^{194} and Asn^{290}). Sequence alignment of $P2X_3$ with the other P2X family members shows a different degree of conservation among these glycosylation sites, with Asn^{139} and Asn^{170} being the more conserved (five and six P2X members, respectively; Figure 1). Remarkably, no single N-glycosylation consensus is conserved within the seven members of the family. Wild-type (WT) and mutated receptors were transiently transfected in HEK293 cells, since this cell line has been previously and successfully used to characterize the properties of $P2X_3$, as well as of other P2X ion channels (Surprenant et al. 2000; Fischer et al. 2003; Jones et al. 2004). We recorded inward current responses at −40 mV, using 100 μM α,β-methylene ATP (αβmeATP) as a ligand. At this concentration, we obtained maximal current responses from WT $P2X_3$ receptor. The currents recorded from the single-mutated N139Q, N194Q and N290Q receptors were found quantitatively identical to those of WT, indicating that none of these three glycans was essential for functional expression. Conversely, N170Q mutated receptor exhibited a consistently lower response (~60% reduction; Figure 2A, Table I). In order to evaluate if this reduced current was due to altered function or to reduced PM delivery, we measured the expression of WT and mutated receptors at the PM. We performed cell-surface biotinylation of PM proteins using the cell-impermeant reagent Biotin-XX-SE. As shown in Figure 2B and Table I, total and PM expression of mutated receptors resembled what we also observed with inward current measurement: N139Q, N194Q and N290Q single *N*-glycan mutants displayed a level of PM expression similar to WT receptors. N170Q mutant instead exhibited a consistent reduction in both total and PM expression, as well as in inward current (Figure 2A). The percent of PM receptor vs. total protein is relatively low (~15%) for $P2X_3$ receptor due to constitutive endocytosis (Vacca et al., 2009) and is not further decreased in the N170Q mutant compared with control (Figure 2D). These observations suggest that the receptors that do not reach the PM are not accumulating intracellularly and are probably degraded. Since it has been already observed that different mutations in the N-glycosylation consensus (N-X-S/T) can produce different functional effect independently from the effect on glycosylation (Gong et al. 2002), we also mutated Thr^{172} to Ala in the Asn^{170} consensus. Gel analysis (×Figure 2C; Figure 3) confirmed that T172A mutant failed to be glycosylated just as N170Q. The effect of T172A mutation appeared drastically more severe, with respect to N170Q, on both total and PM expression (Figure 2C), as well as on current responses (Figures 2A). As for N170Q, the PM/total protein ration is not significatively altered for the T172A mutant (Figure 2D).

In order to confirm that each individual consensus site is indeed N-glycosylated, we performed complete deglycosylation of protein extracts with *N*-Glycosidase F (PNGase F). As

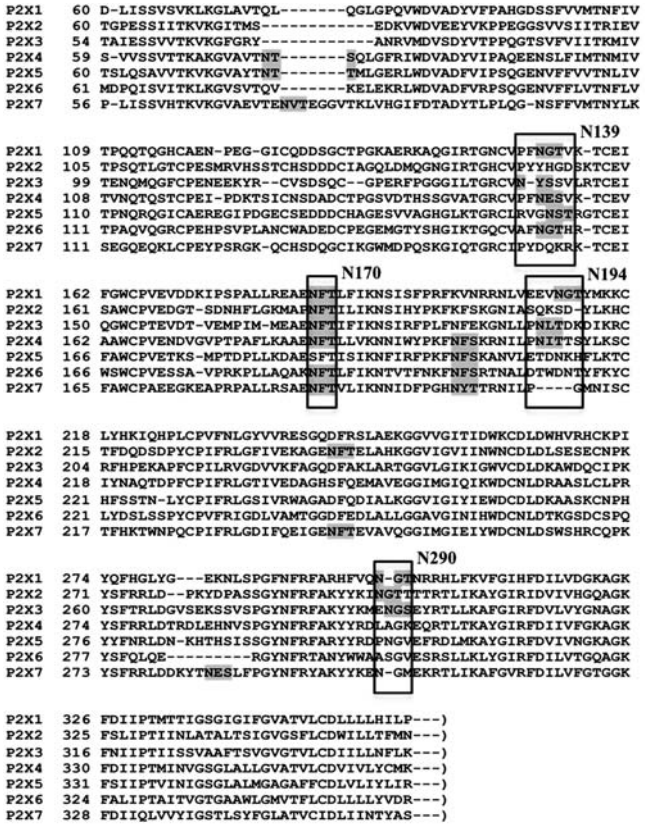

Fig. 1. Alignment of the extracellular portion of rat P2X-family receptors protein sequences. Protein sequences of $P2X_{1-7}$ from rat origin were obtained from UniprotKB database (accession numbers: P47824 ($P2X_1$), P49653 ($P2X_2$), P49654 ($P2X_3$), P51577 ($P2X_4$), P51578 ($P2X_5$), P51579 ($P2X_6$) and Q64663 ($P2X_7$)) and aligned with ClustalW2 software. Consensus sequences for N-glycosylation are highlighted in grey. N-Glycosylation sites of $P2X_3$ (N139, N170, N194 and N290) are indicated.

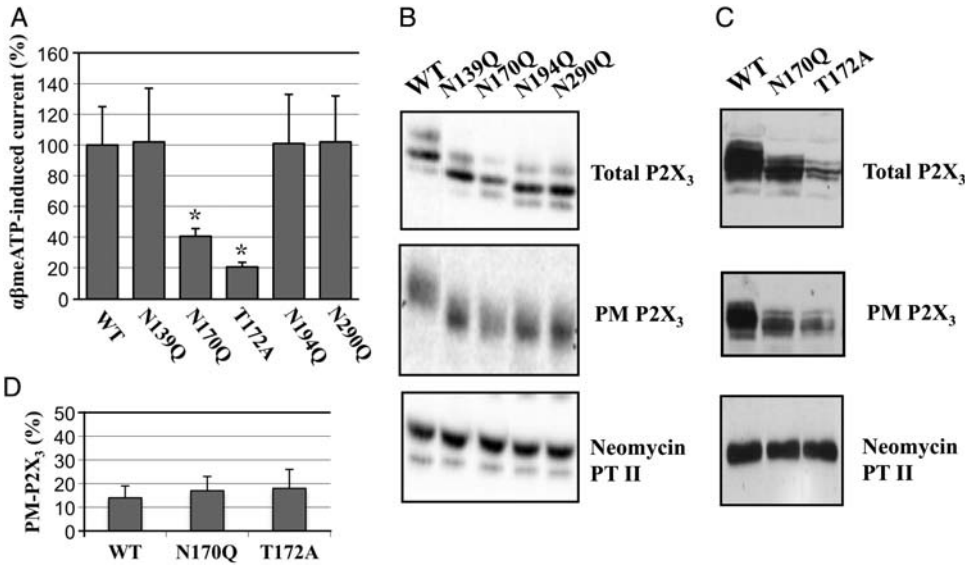

Fig. 2. Effect of single mutation of N-glycosylation sites on functional expression of $P2X_3$ receptor. (**A**) Inward currents induced by 100 μM αβmeATP on WT and N-glycosylation site-mutated $P2X_3$ receptor transfected in HEK293 cells. Data represent an average of at least 10 cells recorded for each mutant from three independent transfections. $*P < 0.05$ in Student's *t*-test compared with WT. (**B** and **C**) HEK293 cells, transfected with the indicated mutants, were labeled with the Biotin-XX-SE. Streptavidin precipitated (PM $P2X_3$) and total cell extracts (Total $P2X_3$) were probed with $P2X_3$ antiserum in western blot. The neomycin PT II protein was used to normalize plasmid expression levels. Similar results were obtained in at least three independent experiments. (**D**) Percent streptavidine precipitated. $P2X_3$ (PM) vs. the amounts of $P2X_3$ in the starting cell lysate for WT and indicated mutant receptors.

Table I. Synoptic view of the effects of single or double mutations of N-glycosylation sites of $P2X_3$ receptor on total protein content, PM expression, percent of receptor present in the trimeric form and inward current

	Tot Prot	PM	Trimer (%)	Current
WT	100	100	81 ± 7	100
N139Q	92 ± 17	85 ± 18	75 ± 17	102 ± 35
N170Q	43 ± 15	55 ± 11	62 ± 11	40.5 ± 5
T172A	28 ± 13	38 ± 7	–	20.5 ± 3
N194Q	85 ± 17	87 ± 13	75 ± 16	101 ± 32
N290Q	89 ± 14	84 ± 15	79 ± 15	102 ± 30
N139Q/N170Q	34 ± 13	23 ± 6	18 ± 5	5 ± 4
N139Q/N194Q	45 ± 9	55 ± 8	72 ± 9	39 ± 20
N139Q/N290Q	28 ± 12	31 ± 12	18 ± 4	0 ± 0
N170Q/N194Q	26 ± 8	14 ± 6	15 ± 6	5.2 ± 3
N170Q/N290Q	20 ± 8	13 ± 5	19 ± 3	3 ± 2
N194Q/N290Q	95 ± 10	102 ± 12	80 ± 5	93.5 ± 29

Data represent the % values ± SD, referred to the control WT $P2X_3$ receptor (100%) for total protein, PM expression and inward current. Total and PM protein levels were normalized to Neomycin PT II protein levels. These data are the average of at least three independent experiments (western blots) or at least 10 cells recorded for each mutant from three independent transfections, $*P < 0.05$ in Student's *t*-test.

shown in Figure 3, all mutants showed the same electrophoretic mobility of WT receptor after PNGase F treatment, indicating that the increased mobility observed in mutants before treatment was due to differential glycosylation status, and not to aberrant effects of amino-acid substitution. Even after extensive PNGase F treatment, $P2X_3$ receptor clearly migrated as a triplet, indicating that this heterogeneity likely depends on post-translational modifications different from N-glycosylation.

The effect of double mutation is strongly dependent on the identity of the mutated N-*glycan*

Differently from single mutants, the majority of double mutations strongly affected receptor expression on its whole and at the PM (Figure 4B). Moreover, as shown in Figure 4A and Table I, N139Q/N170Q, N139Q/N290Q, N170Q/N194Q and N170Q/N290Q mutants elicited very low or null inward currents when stimulated with αβmeATP. Conversely, N139Q/N194Q mutant elicited a considerable, although lower than WT, inward current response (~60% reduction). Only N194Q/N290Q mutant held an inward current indistinguishable from the WT receptor. Similarly to what observed with single mutants, also in double-mutant receptors, there was always a correspondence between current and protein expression levels (Figure 4A and B, Table I). Nevertheless, for those double mutants displaying very low current responses (N139Q/N170Q, N139Q/N290Q, N170Q/N194Q and N170Q/N290Q), a concomitant impairment in ion channel responsiveness cannot be excluded.

EC_{50} is also affected in N170Q and N139Q/N194Q mutants

The single-mutant N170Q and the double-mutant N139Q/N194Q showed a clear reduction in inward current compared with the WT receptor (~40% at 100 μM αβmeATP) that can be mostly attributed to reduced the PM expression of the mutant. In order to better analyze the effect of mutation on channel function, we performed a full dose response on these mutants. As shown in Figure 5, not only I_{max} was significantly decreased, but also EC_{50} of mutants was clearly increased in both mutants, compared with WT (~75%),

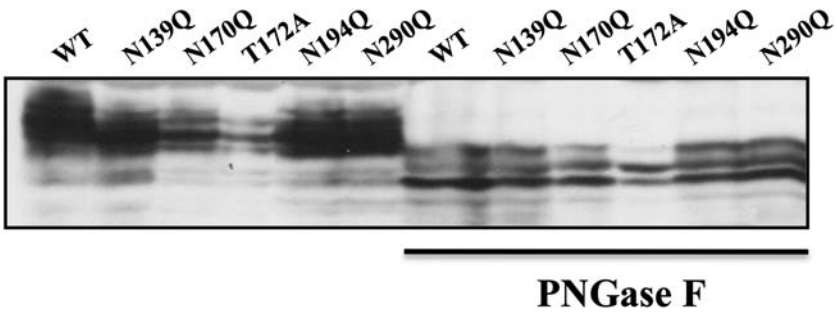

Fig. 3. Effect of deglycosylation with PNGase F on P2X$_3$ receptor mutants gel motility. Cell extracts from HEK293 cells were treated with or without PNGase F (1 U/100 mg of proteins) for 18 h at 37°C and probed with P2X$_3$ antiserum in western blot.

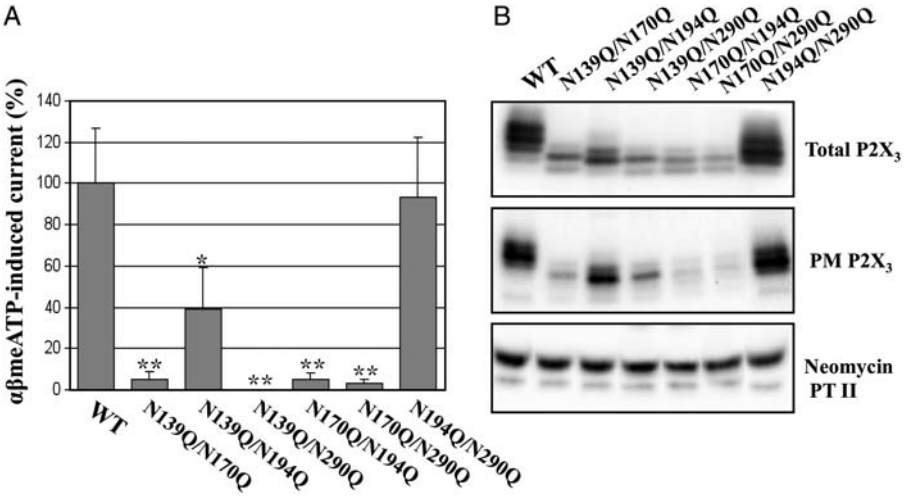

Fig. 4. Effect of double mutation of N-glycosylation sites on functional expression of P2X$_3$ receptor. (**A**) Inward currents induced by 100 μM αβmeATP on WT and N-glycosylation site-mutated P2X$_3$ receptor transfected in HEK293 cells. Data represent an average of at least 10 cells recorded for each mutant from three independent transfections. *$P < 0.05$ in Student's *t*-test compared with WT; **$P < 0.05$ in Student's *t*-test compared with N139Q/N194Q. (**B**) HEK293 cells, transfected with the indicated mutants, were labeled with the Biotin-XX-SE. Streptavidin precipitated (PM P2X$_3$) and total cell extracts (Total P2X$_3$) were probed with P2X$_3$ antiserum in western blot. The neomycin PT II protein was used to normalize plasmid expression levels. Similar results were obtained in at least three independent experiments.

indicating that the mutations generated also a defect in ligand affinity and not only in trafficking of the receptor.

Nonfunctional-mutated receptors do not form appreciable levels of trimers

Blue native (BN) gel electrophoresis was performed in order to evaluate the ability of *N*-glycan mutants of P2X$_3$ receptor to form trimers, the functional oligomer for this receptor subtype. Whereas all single mutants were mainly detected in their trimeric form, the amount of trimer was strongly reduced in the N170Q mutant, consistently with reduced content of total and PM receptor protein (Figure 6, Table I). Also the functional *N*-glycan double mutants N139Q/N194Q and N194Q/N290Q were expressed as trimers, whereas the four not functional double mutants N139Q/N170Q, N139Q/N290Q, N170Q/N194Q and N170Q/N290Q were instead detected mainly as dimers and monomers. This result would indicate that deficiency in trimeric formation might be caused not only by the overall reduced expression of mutated P2X$_3$ protein, but also by the direct inability of *N*-glycan double mutants to correctly oligomerize.

Inhibition of 26S proteasome rescues the content of mutated receptors but not the trimer formation

The role of *N*-glycans in the proper folding and 26S proteasome-dependent degradation of glycoproteins is well documented (Meusser et al. 2005). We thus hypothesized that the reduced level of expression of selected double glycosylation mutants might be due to improper folding and consequent degradation of the mutated receptors. After treating the cells with the 26S proteasome inhibitor MG132 for 7 h, we observed that total and PM protein levels consistently increased in all double-mutated receptors (Figure 7). Moreover, especially in MG132-treated cells, we observed the accumulation of a P2X$_3$ immunoreactive band of 75–80 kDa, likely corresponding to the poly-ubiquitinated form of the receptor, as recognized by anti-ubiquitine antibodies (data not shown). The same band was moreover abolished performing

A

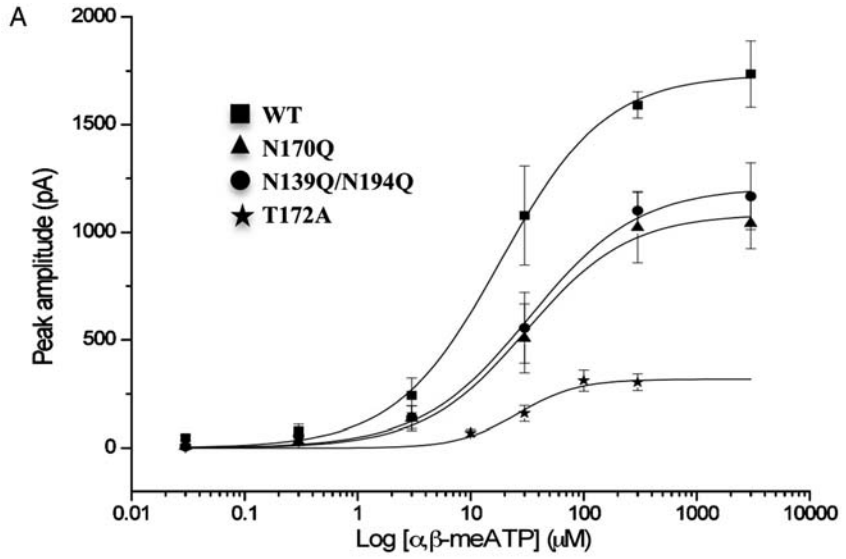

B

	EC_{50}	I_{MAX}	Hill coefficient
WT	18.40 ± 2.18	1733.58 ± 40.77	0.94 ± 0.09
N170Q	30.93 ± 5.90	*1085.66 ± 45.38	0.96 ± 0.17
N139Q/N194Q	32.99 ± 5.50	*1209.88 ± 43.33	0.91 ± 0.12
T172A	26.16 ± 4.27	*317.54 ± 16.06	1.64 ± 0.41

Fig. 5. Concentration-response curves of αβmeATP (0.03–3000 μM) in HEK293 cells transfected with the WT P2X3 receptor (WT) and with its mutants (N170Q, N139/N194Q and T172A). αβmeATP was pressure applied for 2 s in the close proximity to the recorded cell. Data are reported as the mean ± SEM (n = 4–16 cells for each agonist concentration) and are fitted using the Hill equation (see *Materials and Methods* for details). For T172A mutant, we did not calculate the response current at 3000 μM concentration because 100 and 300 μM αβmeATP already produced the maximal response. (**B**) Synoptic view of the effects of single and double mutations of N-glycosylation sites of P2X3 receptor on EC_{50}, I_{max} and Hill coefficient. Data are reported as the mean ± SEM. *P < 0.05 relative to WT in unpaired Student's t-test.

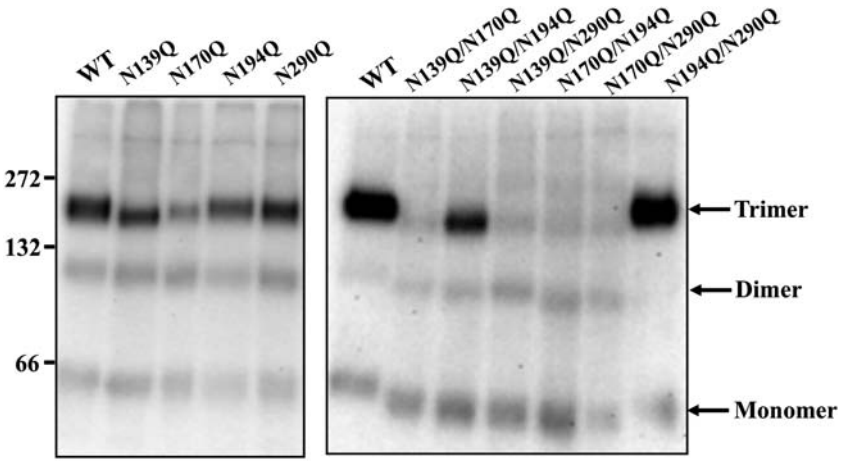

Fig. 6. Oligomeric structure of N-glycosylation site-mutated $P2X_3$ receptor. HEK293 were transiently transfected with WT and the indicated mutant $P2X_3$ receptors. Cell extracts were analyzed by BN gel electrophoresis in order to analyze the oligomeric structure of the receptor. Similar results were obtained in at least three independent experiments.

immunoreactions in the presence of the $P2X_3$ receptor specific immunogenic peptide (data not shown). The 75–80 kDa band was also highly reduced from PM fractions (Figure 7), therefore indicating that ubiquitination of the receptor was scarcely compatible with recruiting at the PM. Finally, treatment with MG132 increased oligomerization mainly in WT,

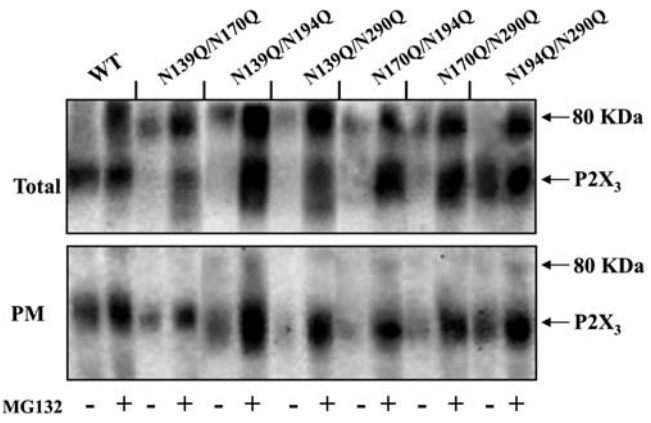

Fig. 7. Role of 26S proteasome inhibition on overall and PM expression of N-glycosylation site-mutated P2X$_3$ receptor. HEK293 were transiently transfected with WT and the indicated mutant P2X$_3$ receptors. Cells were treated in the presence (+) or the absence (−) of 5 μM MG132 for 7 h, and protein extracts were analyzed by SDS–PAGE–western blot for total and PM P2X$_3$ receptor protein. Similar results were obtained in at least three independent experiments.

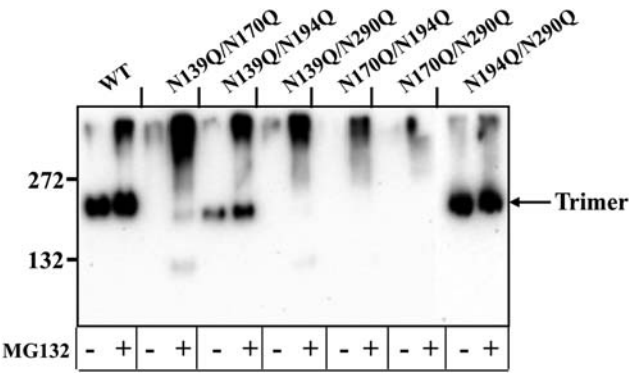

Fig. 8. Role of 26S proteasome inhibition on oligomerization of N-glycosylation site-mutated P2X$_3$ receptor. HEK293 cells were transiently transfected with WT and the indicated mutant P2X$_3$ receptors. Cells were treated in the presence (+) or the absence (−) of 5 μM MG132 for 7 h. Cell extracts were analyzed by BN gel electrophoresis in order to analyze oligomeric structure of the receptors. Similar results were obtained in at least three independent experiments.

N194Q/N290Q and N139Q/N194Q receptors, the only mutants to be already present as trimers under basal conditions (Figure 8). Those double mutants totally unable to trimerize (N139Q/N170Q, N139Q/N290Q, N170Q/N194Q and N170Q/N290Q) instead failed to assemble in oligomeric structures, even in the presence of MG132, but formed a remarkably high molecular weight smeared protein complex, likely corresponding to multi-aggregated forms of the receptor also protected from degradation.

Discussion

The results presented in this work provide direct evidence about the role of N-glycosylation in some different steps that lead to the functional expression of P2X$_3$ receptor on the cell surface. We demonstrated that the predicted glycosylation sites Asn^{139}, Asn^{170}, Asn^{194} and Asn^{290}, which are homologous to the established glycosylated sites of P2X$_1$ receptor (Rettinger et al. 2000), are indeed glycosylated in vivo, as revealed by the shift in molecular weight observed in every single mutant. Nonetheless, a diverse degree of stringency pertains to the different *N*-glycan residues toward overall protein stability, PM delivery, trimer formation and inward current response. The three N-glycosylation residues Asn^{139}, Asn^{194} and Asn^{290} are apparently dispensable for functional expression of P2X$_3$ protein (single mutations still allowed maximal inward current and proper trimeric folding), although our analysis cannot exclude that fully responsive mutated receptors could still elicit less obvious changes in biochemical or electrophysiological properties. Instead, N-glycosylation residue Asn^{170} is found necessary for full overall and PM receptor expression, proper oligomerization and current response. The increase in EC$_{50}$ compared with WT clearly indicates a reduced ligand affinity of the N170Q mutant. On the other hand, the reduction in I_{max} (∼62 % of WT, Figure 5) correlates well with that in PM expression (55 ± 11%, Table I), indicating that the mutant receptors reaching the PM are likely functional.

However, Asn^{170} is not the only essential glycosylation residue, since also double mutation of Asn^{139} and Asn^{290} residues caused complete improper folding and functional loss. Contemporary mutation of either combination of three glycosylation sites or treatment of cells with tunicamycin completely impairs the PM expression of the receptor (not shown) indicating that a certain degree of glycosylation is necessary for receptor functional assembly.

High-resolution crystal structure of the zebrafish P2X$_{4.1}$ receptor has been recently solved (Kawate et al. 2009). Of the four glycosylation sites of the rat P2X$_3$ receptor, Asn^{139} and Asn^{290} are not conserved in zebrafish P2X$_{4.1}$, Asn^{194} is not strictly conserved but a new consensus is present and shifted by only two amino acids, whereas Asn^{170} is conserved. When superimposing the rat P2X$_3$ sequence to the P2X$_4$ structure, all four glycosylated asparagines lie in exposed regions of the molecule. Interestingly, the homologous of Asn^{170} (Asn^{187} in P2X$_4$) is placed very near to the cavity proposed to bind ATP with Thr of the consensus site (Thr^{189} in P2X$_4$) directly taking part in nucleotide binding. This observation could explain the stronger effect of Asn^{170} mutation on P2X$_3$ receptor function compared with the other glycosylation mutants and also the more dramatic effect of the Thr^{172} mutation (homologous to Thr^{189} in P2X$_4$) with respect to Asn^{170}. Differently from the N170Q mutant, the reduction in the I_{max} of the T172A mutant (∼18% of WT, Figure 5) is significantly more severe than that in PM expression (38 ± 7%, Table I), thus suggesting also a partial functional impairment of the receptor pool reaching the PM. Functional impairments have been indeed already observed when mutating the homologous Thr in P2X$_1$ (Roberts and Evans 2006) and P2X$_2$ (Jiang et al. 2000) receptors. Moreover, the homologous of Asn^{170} is also critical for PM trafficking and function of P2X$_7$ receptor (Lenertz et al. 2010).

Our data also confirm the results obtained by a similar analysis of *N*-glycan mutations on the functional expression

of $P2X_1$ protein (Rettinger et al. 2000). Yet, the effects that we observed with $P2X_3$ receptor were consistently more pronounced, especially in the case of the double mutants, and the residue Asn^{184} in the $P2X_1$ receptor (homologous to Asn^{170} in $P2X_3$) seemed to be less critical (Rettinger et al. 2000), therefore signifying that the $P2X_3$ receptor subtype is probably more dependent than $P2X_1$ upon *N*-glycans for proper assembly, trafficking and function. This diversity might also be due to variation in the cell systems and species adopted, since the work on $P2X_1$ was performed in *Xenopus* oocytes. Indeed, in the same HEK293 cellular system, the importance of *N*-glycans for proper functioning of $P2X_3$ receptors was already recognized, since only fully N-glycosylated receptors responded to external pH with a modified sensitivity toward αβmeATP, and the absence of individual *N*-glycans modified the pH sensitivity, most probably by an allosteric mechanism (Wirkner et al. 2008). Again in HEK293 cells, *N*-glycan double-mutation studies performed on $P2X_2$ (Torres et al. 1998) provided more similar results to ours on $P2X_3$. Although in the absence of systematic mutagenesis of all individual N-glycosylation sites, studies carried out on $P2X_4$ (Hu et al. 2002) and $P2X_6$ (Jones et al. 2004) receptors again confirmed our results indicating the crucial role of *N*-glycans in the full functional expression of this entire family of ionotropic receptors.

It is well known that misfolded proteins are eliminated by a process called ER-associated degradation. Basically, proteins are back translocated from ER into the cytosol and then degraded by the 26S proteasome (Meusser et al. 2005). P2X receptors are well known to be present as trimers in the ER, meaning that they assemble in trimeric structures early in the biosynthetic pathway (Nicke et al. 1998). The relationship between oligomerization and degradation is nevertheless still unclear. With our studies, we recognized that inhibition of the 26S proteasome leads to accumulation of both WT and all double-mutated receptors and that total content of whole and PM $P2X_3$ receptor is comparable in WT vs. double mutants in the presence of proteasome inhibitor. These results indicated that the observed low levels of mutant proteins were probably due to proteasome-dependent degradation. This was also confirmed by the ubiquitous presence (significantly not at the PM) of a 75–80 kDa poly-ubiquitinated $P2X_3$ protein signal. It is not clear yet to what extent the various sequential steps of the degradation process are linked to one another (Elkabetz et al. 2004). Major histocompatibility complex class I and T-cell receptors are known to accumulate in the cytosol when proteasomal degradation is inhibited (Wiertz et al. 1996; Yu et al. 1997). Instead, for other proteins such as the immunoglobulin moieties, dislocation and proteasomal function appear to be strictly linked, since it has been observed that proteasomal blockade can cause the retention of these proteins in the ER membrane (Chillaron and Haas 2000; Mancini et al. 2000). After proteasomal inhibition, the consistent increase in all mutated $P2X_3$ proteins reaching the PM therefore indicates not only that mutated receptors are protected from back translocation to the cytosol, but also that mutated $P2X_3$ receptors can progress through the entire secretory pathway. Conversely, when we looked at oligomerization of WT vs. mutated receptors, we found that inhibition of the 26S proteasome increases the trimeric form of the receptor, when this is less abundant (N139Q/N194Q), while having a moderate effect on WT and N194Q/N290Q mutant. In the other mutated receptors (N139Q/Asn^{170}, N139Q/N290Q, N170Q/N194Q and N170Q/N290Q) in which the trimers were barely detectable under basal conditions, these are not present also after 26S proteasome inhibition, indicating that these mutants are likely not competent for trimer formation. This would signify that complete trimerization is prevented by early degradation in the N139Q/N194Q mutant even if this mutant is still competent for trimerization. This is also confirmed by the observation that, even in the presence of lower levels of protein, the percent of receptor present in the trimeric form is only slightly lower than WT for both N170Q and N139Q/N194Q mutants.

In synthesis, we demonstrated here that the six different possible combinations of *N*-glycan double mutants of $P2X_3$ protein differently influence oligomerization and functional expression of the receptor and induce various extents of receptor degradation. By comparative analysis, we moreover established a diverse degree of stringency in the different *N*-glycans, with Asn^{170} that appears to be the most important site for receptor proper folding and stability, since its single or joint mutation caused the most severe impairments. Consistently, this is the best conserved glycosylation site within the P2X family and the recently solved crystal structure of $P2X_4$ places this residue very close to the putative ATP binding site (Kawate et al. 2009). Asn^{194} and Asn^{290} were instead the most dispensable, as their simultaneous mutation did not apparently affect any receptor feature. All remaining double mutants elicited progressively more severe impairments. When proteasomal degradation was instead inhibited, whereas full receptor stability and trafficking to the PM was restored for all the combinations of *N*-glycan double mutants, trimerization was only selectively permitted, therefore indicating that folding impairments cannot be overcome by receptor stabilization.

In conclusion, these results improve our knowledge about the role of N-glycosylation in proper folding and oligomeric association of $P2X_3$ receptor. A new emerging finding is that the inability to assemble into trimers might account for the impaired function in mutants where residue Asn^{170} is replaced. This might shed light on a novel mechanism eventually responsible for malfunctioning of this receptor during pathological conditions.

Materials and methods

Cell cultures, transfections and treatments

The human HEK293 cell line was cultured in Dulbecco's modified Eagle's medium (Sigma, Milano, IT), supplemented with 2 mM L-glutamine, 100 U/mL of penicillin, 100 µg/mL of streptomycin and 10% heat inactivated calf serum (Invitrogen, San Giuliano Milanese, Italy). Cells were transfected with full-length cDNA coding for $P2X_3$ WT and mutated receptors inserted in the pcDNA3 vector (Invitrogen); control cells were transfected with the empty pcDNA3 vector. Cells were transfected at 80–90% confluence in 35 mm wells with 5 µL of lipofectamine 2000 reagent (Invitrogen) and

4 μg of plasmid DNA, according to the manufacturer's instructions. The medium was replaced after 4 h and experiments were performed ~24 h later. Similar results were obtained when experiments were performed 48 h after transfection even if the expression level was already slightly declining compared with 24 h.

Site-directed mutagenesis

Asn-coding triplets in the four N-glycosylation consensus sequences in the rat $P2X_3$ cDNA were substituted with Gln-coding triplets by two-step overlapping polymerase chain reaction site-directed mutagenesis, essentially as described (Ho et al. 1989).

The following primers were used for the mutations: N139Q (for-GGCCGCTGCGTGCAATACAGCTCTGTT; rev-CCGG AGAACAGAGCTGTATTG CACGCA); N170Q (for-CATGA TGGAGGCTGAGCAATTCACCAT; rev-TGATGAAA ATGG TGAATTGCTCAGCCT); N194Q (for-GGGAAACCTCCTG CCTCAACTCACCGA; rev-CTTGTCGGTGAGTTGAGGCA GGAGGTT); N290Q (rev-CTATAAGATGGAGCAAGGCA GCGAGTA; rev-TACTCGCTGCCTTGCTCCATCTTATAG) and T172A (for-GGAGGCTGAGAACTTCGCCATTTTCA TCAAGAAC; rev-GTTCTTGATGAAAATGGCGAAGTTC TCAGCCTCC). Double mutants were produced introducing a second mutation on a previously obtained single-mutated template. All mutations and the lack of secondary mutation eventually introduced in the amplification steps were verified by sequencing on both strands.

Electrophysiological recordings

For electrophysiological experiments, HEK293 cells were plated on glass coverslips and cotransfected with $P2X_3$ plasmid and a green fluorescent protein (GFP) expressing plasmid (Invitrogen; 1:8 molar ratio). Coverslips were placed in a recording chamber, on the stage of an upright microscope (Axioscope FS, Carl Zeiss, Germany) equipped for infrared video microscopy (Hamamatsu, Hamamatsu City, Japan) and submerged in a continuously flowing (2.5 mL/min) solution at room temperature (20–22°C). This solution contained (in mM) 126 NaCl, 2.5 KCl, 1.2 $MgCl_2$, 1.2 NaH_2PO_4, 2.4 $CaCl_2$, 10 glucose and 18 $NaHCO_3$, gassed with 95% O_2 and 5% CO_2. Whole-cell patch clamp recordings were obtained from GFP positive cells visualized by epifluorescence at 480 ± 40 nm excitation wavelength at an holding potential of −40 mV. Borosilicate glass electrodes (WPI 1.5 mm) were pulled with a PP 83 Narishige puller. The resistance of the pipette was ~4 MΩ when filled with a standard solution containing (in mM) 145 KCl-gluconate, 0.1 $CaCl_2$, 2 $MgCl_2$, 10 4-(2-Hydroxyethyl)-1-piperazineethanesulfonic acid, 0.75 [Ethylenebis(oxyethylenenitrilo)]tetraacetic acid, 2 Mg-ATP, and 0.3 Na_3GTP, pH 7.3. The membrane voltage and current were acquired using pClamp and Axoscope software (Axon Instruments, Sunnyvale, CA). Agonist (100 μM αβmeATP) was applied via a patch pipette that was positioned in close vicinity of the cell body and was connected to a pressure application system (Picospritzer, 20–30 psi, 0.1–10 s).

Concentration response curves of αβmeATP (0.03–3000 μM) were obtained by pressure application of each agonist concentration to a group of 4–16 cells. Data were fitted using the Hill equation:

$$I = \frac{I_{max}}{1 + (EC_{50}/x)^n}$$

where I is the peak current produced by the agonist, I_{max} the maximal current at saturating agonist concentration, n the Hill coefficient and EC_{50} the concentration of the agonist producing 50% of I_{max}.

Surface biotinylation and isolation of biotinylated proteins

After transfection (24 h), HEK293 cells were washed twice with Dulbecco's modified phosphate-buffered saline (D-PBS) containing 0.6 mM $MgCl_2$ and 1.8 mM $CaCl_2$. Surface proteins were biotinylated incubating the cells with 0.5 mg/mL of 6-((6-((biotynoyl)amino)hexanoyl)amino)-hexanoic acid, succinimidyl ester (Biotin-XX-SE) (Invitrogen) dissolved in D-PBS containing 0.6 mM $MgCl_2$ and 1.8 mM $CaCl_2$ for 30 min at 4°C. Cells were then washed three times with D-PBS and lysed with lysis buffer (10 mM Tris–HCl, pH 7.5, 150 mM NaCl, 1% Triton X-100, 2 mM ethylenediaminetetraacetate, 1 mM phenylmethylsulfonyl fluoride, 20 μM leupeptin) and centrifuged at 15000 × *g* for 10 min at 4°C. Cell lysates were quantified for protein content by the Bradford method (Bio-Rad Laboratories, Segrate, Italy) and normalized lysate volumes were used. Biotinylated proteins were precipitated by incubating lysates with streptavidin-coupled agarose beads (Invitrogen) for 2 h at 4°C. Beads were then washed three times with lysis buffer and then boiled for 5 min after the addition of 2× Laemmli sample buffer (15 μL/sample). Proteins were separated on sodium dodecyl sulfate-polyacrylamide gel electrophoresis (SDS-PAGE).

Protein deglycosylation with PNGase F

For PNGase F studies, total cell lysates (100 μg/condition) were adjusted to a final concentration of 0.2% SDS and 1% β-mercaptoethanol, treated 10 min at 95°C and incubated 18 h at 37°C, with or without 1 U of PNGase F (Roche Diagnostics, Mannheim, Germany). Proteins were then separated on SDS–PAGE.

SDS–PAGE and BN–PAGE electrophoresis and immunoblotting

For SDS–PAGE, cellular lysates were diluted in 4× Laemmli sample buffer, containing a final concentration of 2% (vol/vol) β-mercaptoethanol as reducing agent, and proteins were separated on 7.5 or 12.5% polyacrylamide gels. For BN gels, cells were lysed in BN-lysis buffer (50 mM Bis–Tris, pH 7, 1% *N*-dodecyl maltoside, 10% glycerol, 0.75 M aminocaproic acid). Cellular lysates were kept on ice for 30 min and then centrifuged for 10 min at 14000 × *g* at 4°C. Supernatants were collected and quantified. BN–PAGE was carried out essentially as described (Schagger and Jagow 1991). After incubation for 1 h at 37°C with 0.1% SDS, proteins were run on 8–14% gradient gels. Blotting to nitrocellulose membranes (Amersham Biosciences, Milano, Italy) was performed using Tris–glycine transfer buffer with 20% (vol/vol) CH_3OH. Not specific binding was prevented by incubating the blotted

membranes in 5% (wt/vol) not fat dry milk in TBS-T (tris-buffered saline, 0.2% (vol/vol) Tween-20). Primary antibodies were incubated for 2 h at room temperature (neomycin phosphotransferase II, 1:1000, purchased from Upstate, Billerica, MA) or overnight at 4°C ($P2X_3$, purchased from Alomone, Jerusalem, Israel). Secondary peroxidase–conjugated antibodies were used for 50 min at room temperature. The antibodies were diluted in TBS-T with 3% (wt/vol) not fat dry milk. Immunostained bands were visualized using the ECL detection system (Amersham Biosciences) acquired with Kodak 440CF Image Station; band intensities were measured with 1D image analysis software (Eastman Kodak Company, Rochester, NY). PM to total ratios of WT and mutant $P2X_3$ receptors were estimated by comparing scalar amounts of starting cell lysate with streptavidine precipitate as described previously (Vacca et al. 2009).

Statistical analysis

Numerical data in bar graphs and table are expressed as the mean ± SD. Unpaired Student's *t*-test was used to compare data and $P < 0.05$ was considered significant.

Funding

This work was supported by Ministry of Health Grant Fondazione Santa Lucia [RC2009–11C].

Conflict of interest

None declared.

Abbreviations

αβmeATP, α,β-methylene ATP; BN, blue native; D-PBS, Dulbecco's modified PBS; ER, endoplasmic reticulum; GFP, green fluorescent protein; PM, plasma membrane; PNGase F, *N*-Glycosidase F; TBS, tris-buffered saline; WT, wild type.

References

Barrera NP, Ormond SJ, Henderson RM, Murrell-Lagnado RD, Edwardson JM. 2005. Atomic force microscopy imaging demonstrates that P2X2 receptors are trimers but that P2X6 receptor subunits do not oligomerize. *J Biol Chem*. 280:10759–10765.

Chillaron J, Haas IG. 2000. Dissociation from BiP and retrotranslocation of unassembled immunoglobulin light chains are tightly coupled to proteasome activity. *Mol Biol Cell*. 11:217–226.

Cockayne DA, Hamilton SG, Zhu QM, Dunn PM, Zhong Y, Novakovic S, Malmberg AB, Cain G, Berson A, Kassotakis L, et al. 2000. Urinary bladder hyporeflexia and reduced pain-related behaviour in P2X3-deficient mice. *Nature*. 407:1011–1015.

Daniels R, Kurowski B, Johnson AE, Hebert DN. 2003. N-linked glycans direct the cotranslational folding pathway of influenza hemagglutinin. *Mol Cell*. 11:79–90.

De Souza NF, Simon SM. 2002. Glycosylation affects the rate of traffic of the Shaker potassium channel through the secretory pathway. *Biochemistry*. 41:11351–11361.

Elkabetz Y, Shapira I, Rabinovich E, Bar-Nun S. 2004. Distinct steps in dislocation of luminal endoplasmic reticulum-associated degradation substrates: Roles of endoplasmic reticulum-bound p97/Cdc48p and proteasome. *J Biol Chem*. 279:3980–3989.

Fischer W, Wirkner K, Weber M, Eberts C, Koles L, Reinhardt R, Franke H, Allgaier C, Gillen C, Illes P. 2003. Characterization of P2X3, P2Y1 and P2Y4 receptors in cultured HEK293-hP2X3 cells and their inhibition by ethanol and trichloroethanol. *J Neurochem*. 85:779–790.

Freeze HH. 2001. Update and perspectives on congenital disorders of glycosylation. *Glycobiology*. 11:129R–143R.

Gehle VM, Walcott EC, Nishizaki T, Sumikawa K. 1997. N-glycosylation at the conserved sites ensures the expression of properly folded functional ACh receptors. *Brain Res Mol Brain Res*. 45:219–229.

Gong Q, Anderson CL, January CT, Zhou Z. 2002. Role of glycosylation in cell surface expression and stability of HERG potassium channels. *Am J Physiol Heart Circ Physiol*. 283:H77–H84.

Hebert DN, Garman SC, Molinari M. 2005. The glycan code of the endoplasmic reticulum: Asparagine-linked carbohydrates as protein maturation and quality-control tags. *Trends Cell Biol*. 15:364–370.

Ho SN, Hunt HD, Horton RM, Pullen JK, Pease LR. 1989. Site-directed mutagenesis by overlap extension using the polymerase chain reaction. *Gene*. 77:51–59.

Hu B, Senkler C, Yang A, Soto F, Liang BT. 2002. P2X4 receptor is a glycosylated cardiac receptor mediating a positive inotropic response to ATP. *J Biol Chem*. 277:15752–15757.

Jaeken J, Carchon H. 2004. Congenital disorders of glycosylation: A booming chapter of pediatrics. *Curr Opin Pediatr*. 16:434–439.

Jiang LH, Rassendren F, Surprenant A, North RA. 2000. Identification of amino acid residues contributing to the ATP-binding site of a purinergic P2X receptor. *J Biol Chem*. 275:34190–34196.

Jones CA, Vial C, Sellers LA, Humphrey PP, Evans RJ, Chessell IP. 2004. Functional regulation of P2X6 receptors by N-linked glycosylation: Identification of a novel alpha beta-methylene ATP-sensitive phenotype. *Mol Pharmacol*. 65:979–985.

Kawate T, Michel JC, Birdsong WT, Gouaux E. 2009. Crystal structure of the ATP-gated P2X(4) ion channel in the closed state. *Nature*. 460:592–598.

Khakh BS, North RA. 2006. P2X receptors as cell-surface ATP sensors in health and disease. *Nature*. 442:527–532.

Kowarik M, Kung S, Martoglio B, Helenius A. 2002. Protein folding during cotranslational translocation in the endoplasmic reticulum. *Mol Cell*. 10:769–778.

Lenertz LY, Wang Z, Guadarrama A, Hill LM, Gavala ML, Bertics PJ. 2010. Mutation of putative N-linked glycosylation sites on the human nucleotide receptor P2X7 reveals a key residue important for receptor function. *Biochemistry*. 49:4611–4619.

Mancini R, Fagioli C, Fra AM, Maggioni C, Sitia R. 2000. Degradation of unassembled soluble Ig subunits by cytosolic proteasomes: Evidence that retrotranslocation and degradation are coupled events. *FASEB J*. 14:769–778.

Meusser B, Hirsch C, Jarosch E, Sommer T. 2005. ERAD: The long road to destruction. *Nat Cell Biol*. 7:766–772.

Molinari M, Helenius A. 2000. Chaperone selection during glycoprotein translocation into the endoplasmic Reticulum. *Science*. 288:331–333.

Nicke A, Baumert HG, Rettinger J, Eichele A, Lambrecht G, Mutschler E, Schmalzing G. 1998. P2X1 and P2X3 receptors form stable trimers: A novel structural motif of ligand-gated ion channels. *EMBO J*. 17:3016–3028.

North RA. 2004. P2X3 receptors and peripheral pain mechanisms. *J Physiol*. 554:301–308.

Rettinger J, Aschrafi A, Schmalzing G. 2000. Roles of individual N-glycans for ATP potency and expression of the rat P2X1 receptor. *J Biol Chem*. 275:33542–33547.

Roberts JA, Evans RJ. 2006. Contribution of conserved polar glutamine, asparagine and threonine residues and glycosylation to agonist action at human P2X1 receptors for ATP. *J Neurochem*. 96:843–852.

Schagger H, von Jagow G. 1991. Blue native electrophoresis for isolation of membrane protein complexes in enzymatically active form. *Anal Biochem*. 199:223–231.

Souslova V, Cesare P, Ding Y, Akopian AN, Stanfa L, Suzuki R, Carpenter K, Dickenson A, Boyce S, Hill R, et al. 2000. Warm-coding deficits and aberrant inflammatory pain in mice lacking P2X3 receptors. *Nature*. 407:1015–1017.

Standley S, Baudry M. 2000. The role of glycosylation in ionotropic glutamate receptor ligand binding, function, and trafficking. *Cell Mol Life Sci*. 57:1508–1516.

Surprenant A, Schneider DA, Wilson HL, Galligan JJ, North RA. 2000. Functional properties of heteromeric P2X(1/5) receptors expressed in HEK cells and excitatory junction potentials in guinea-pig submucosal arterioles. *J Auton Nerv Syst*. 81:249–263.

Torres GE, Egan TM, Voigt MM. 1998. N-Linked glycosylation is essential for the functional expression of the recombinant P2X2 receptor. *Biochemistry*. 37:14845–14851.

Vacca F, Amadio S, Sancesario G, Bernardi G, Volonte C. 2004. P2X3 receptor localizes into lipid rafts in neuronal cells. *J Neurosci Res*. 76:653–661.

Vacca F, Giustizieri M, Ciotti MT, Mercuri NB, Volonté C. 2009. Rapid constitutive and ligand-activated endocytic trafficking of P2X receptor. *J Neurochem*. 109:1031–1041.

Vulchanova L, Riedl MS, Shuster SJ, Buell G, Surprenant A, North RA, Elde R. 1997. Immunohistochemical study of the P2X2 and P2X3 receptor subunits in rat and monkey sensory neurons and their central terminals. *Neuropharmacology*. 36:1229–1242.

Watanabe I, Wang HG, Sutachan JJ, Zhu J, Recio-Pinto E, Thornhill WB. 2003. Glycosylation affects rat Kv1.1 potassium channel gating by a combined surface potential and cooperative subunit interaction mechanism. *J Physiol*. 550:51–66.

Wiertz EJ, Jones TR, Sun L, Bogyo M, Geuze HJ, Ploegh HL. 1996. The human cytomegalovirus US11 gene product dislocates MHC class I heavy chains from the endoplasmic reticulum to the cytosol. *Cell*. 84:769–779.

Wirkner K, Stanchev D, Milius D, Hartmann L, Kato E, Zadori ZS, Mager PP, Rubini P, Nörenberg W, Illes P. 2008. Regulation of the pH sensitivity of human P2X receptors by N-linked glycosylation. *J Neurochem*. 10:1216–1224.

Yu H, Kaung G, Kobayashi S, Kopito RR. 1997. Cytosolic degradation of T-cell receptor alpha chains by the proteasome. *J Biol Chem*. 272:20800–20804.